Investigative Ophthalmology & Visual Science, Vol. 33, No. 5, April 1992
Copyright © Association for Research in Vision and Ophthalmology

Modulation of Outflow Resistance by the Pores of the Inner Wall Endothelium

Mark Johnson,* Andrew Shapiro,* C. Ross Ethier† and Roger D. Kamm*

The juxtacanalicular connective tissue (JCT) is widely believed to generate the bulk of aqueous humor outflow resistance, while the pores of the inner wall endothelium are thought to generate at most 10% of this resistance in humans. However, the hydrodynamic interaction of these two components of the aqueous outflow system, which arises because of their spatial proximity, has only recently been considered. Modelling the JCT as a homogeneously distributed porous material upstream of a low porosity filter (the inner wall endothelium), the pores of the inner wall are found to cause a "funneling effect," in which the aqueous humor flows preferentially through those regions of the JCT nearest the inner wall pores. The bulk of the pressure drop occurs in the immediate proximity of the pores (within three pore radii). This greatly increases the apparent flow resistance of the JCT. For a set of parameters characterizing the normal eye, this enhancement is approximately 30-fold. The conclusion of this study is that changes in inner wall porosity may greatly affect aqueous outflow resistance, despite the low flow resistance of the inner wall pores themselves. Invest Ophthalmol Vis Sci 33:1670–1675, 1992

The source of flow resistance in the aqueous outflow system of normal or glaucomatous eyes has not been definitively established, although each of the components of the outflow pathway have been analyzed to determine whether they might generate significant flow resistance. The openings in the corneoscleral meshwork are much too large to generate a significant flow resistance.[1] Furthermore, it has been noted that a widening of these openings associated with an increase in intraocular pressure is accompanied by a counterintuitive increase in the measured outflow resistance of the outflow system.[2] Porous media analysis of the juxtacanalicular connective tissue (JCT)[3,4] indicated that if the apparent open spaces in this region are not filled with an extracellular matrix gel, the JCT flow resistance would be two orders of magnitude less than the measured flow resistance. In humans, the pores in the inner wall endothelium of Schlemm's canal generate perhaps 10% of the total flow resistance.[5] Schlemm's canal itself only generates significant flow resistance when it is substantially collapsed,[2,6] and the collector channels and aqueous veins recently have been shown to have negligible flow resistance[7] (although there is some conflicting evidence from trabeculotomy studies that suggest 25–50% of the flow resistance may exist in this region).[8] Based on such estimates, it has been suggested[3] that the apparently open spaces in the JCT are filled with an extracellular matrix gel, and that such a gel-filled JCT is likely to be the major source of flow resistance in the normal eye.

In general, these models for flow resistance have considered a single component of the aqueous outflow system without considering possible hydrodynamic interactions between neighboring components. In the present study, we consider the JCT and inner wall of Schlemm's canal as a coupled system and include the effects of interactions between the inner wall pores and flow through the JCT. This interaction arises because the pores in the inner wall endothelium are small and well separated. Thus, the distribution of flow within the JCT is unlikely to be uniform as assumed in previous models.[3,4] Rather, flow will be preferentially directed through those regions of the JCT in the vicinity of a pore, reducing the effective cross-sectional area available for the flow of aqueous humor.[9] As will be seen, this "funneling" interaction markedly increases the effective resistance of the JCT and implies that the number and size of pores in the inner wall endothelium might significantly alter total outflow resistance.

*From the Massachusetts Institute of Technology, Cambridge, Massachusetts, and the †University of Toronto, Toronto, Canada.

Supported in part by the National Eye Institute (R01-EY-05503) and Medical Research Council of Canada grant MA10051.

Submitted for publication: August 5, 1991; accepted November 3, 1991.

Reprint requests: Mark Johnson, Department of Mechanical Engineering, Room 3-160, Massachusetts Institute of Technology, 77 Massachusetts Avenue, Cambridge, MA 02139.

To model this situation, the JCT is treated as a porous material[3,4] overlying an impermeable substrate containing pores (the inner wall endothelium). A similar problem was analyzed by Ethier and Kamm[10] using Darcy's law[11] to investigate the flow resistance of a porous filter cake (eg, macromolecular layer) resting on a rejecting membrane (eg, Nucleopore polycarbonate filter). They found that membrane porosity can have a strong effect on the effective flow resistance of such a system. However, they did not examine cases of extremely low membrane porosity appropriate for the inner wall endothelium ($\epsilon \approx 0.001$; see below). In the present study, we extended their analysis using a numerical solution of Darcy's law and develop an analytical solution in the limit of very low inner wall porosity. We found that the average distance between pores in the inner wall endothelium can dramatically affect JCT flow resistance.

Methods

We consider the JCT to be a homogeneous and isotropic porous material of thickness L with flow entering uniformly at its proximal surface ($z = L$) and passing through to pores located at its distal surface ($z = 0$) (the inner wall of Schlemm's canal) (Fig. 1). The inner wall is assumed to have uniformly spaced pores of radius a, density (pores per unit area of inner wall) n, and center-to-center spacing $b = 1/\sqrt{n}$. It is convenient to introduce the inner wall porosity, ϵ, defined as the fraction of inner wall area occupied by pores:

$$\epsilon = n\pi a^2 = \pi a^2/b^2 \tag{1}$$

For the purposes of the flow analysis, it is sufficient to analyze the region surrounding a single pore, having dimensions $b \times b \times L$, as outlined by the dashed lines in Figure 1.

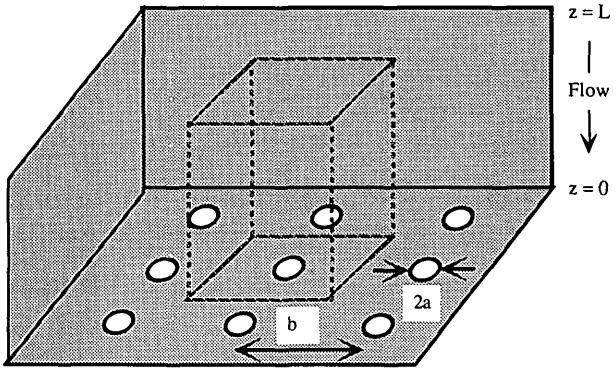

Fig. 1. Computational domain showing the dimensions of the unit cell (bounded by the dashed lines) used in the analysis. The JCT fills the region between z = 0 and z = L.

The flow through the porous JCT is modelled using Darcy's law:[11]

$$\nabla P = \frac{\mu \vec{v}}{K} \tag{2}$$

where P is the pressure, μ the fluid viscosity, K the hydrodynamic permeability of the JCT, and $\vec{v}$ the superficial fluid velocity (flow rate per unit area). To solve this equation, we require boundary conditions on pressure found in the Appendix. Uniform pressure ($P_{sc} + \Delta P$) was specified at the entrance to the JCT, while the pressure at the pore mouth was specified as P_{sc} (pressure in Schlemm's canal). The continuity equation (conservation of mass) is introduced:

$$\nabla \cdot \vec{v} = 0 \tag{3}$$

which, when combined with equation (2), yields Laplace's equation for the pressure distribution:

$$\nabla^2 P = 0 \tag{4}$$

We used the spectral element code NEKTON[12] to numerically solve equation (4) with appropriate boundary conditions (A1–A5). The parameter-space investigated is shown in Table 1.[13,14] Note that the solution of equation (4) for pressure distribution does not require that the JCT permeability be known; it only requires that the JCT can be treated as a porous material in which the flow obeys equation (2). This assumption has been shown to be valid for a wide range of connective tissues.[15]

After the pressure distribution within the JCT is determined, equation (2) can be used to find the velocity distribution and hence the flow rate through the JCT (Q). The resistance (R) of the JCT/inner wall complex is then determined by dividing the total imposed pressure drop across the JCT (ΔP) by Q: $R = \Delta P/Q$. A "resistance enhancement factor" E is defined as:

$$E = \frac{R}{R_0} \tag{5}$$

where $R_0 = \mu L/KA$ is the flow resistance of the JCT alone, if the fluid were not forced to funnel through the pores of the inner wall (A is the cross-sectional area facing flow). E, therefore, measures to what extent the flow resistance of the JCT increases as a result of the presence of the inner wall pores. R_0 also is used to determine a normalized pressure ($\hat{P}$):

$$\hat{P} = \frac{P - P_{sc}}{R_0 Q} = \frac{P - P_{sc}}{\Delta P_0} \tag{6}$$

where ΔP_0 is the pressure drop that would be gener-

Table 1. Range of parameters simulated in the current study*

Parameter	*Typical value*	*Range*	*Comment*
Length of JCT (L)	10 μm	8–16 μm	Ref. 13
Pore diameter (2a)	1 μm	0.1–3 μm	Ref. 5
Pore density (n)	1500 pores/mm^2	1000–2000 pores/mm^2	Ref. 14
Interpore spacing (b)	25 μm	20–30 μm	From n
Porosity (ϵ)	0.001	0.0002–0.02	Equation (1)

* The typical values were selected as representative and used as the baseline case shown in Figures 2 and 3.

ated by the JCT in absence of the inner wall at the same flow rate.

Analytic Limit

An approximate analytic solution to equations (4), (A1–A5) is possible for the case of very small pore size ($a \ll L$, $a \ll b$). Because Laplace's equation (4) also is satisfied by an electrostatic potential, we used the solution for the potential surrounding an isolated conducting circular disk (equivalent to the constant pressure pore) bounded by a semi-infinite space to find:[16]

$$\Delta P = \frac{\mu Q}{4Ka} \tag{7}$$

This solution does not include effects due to the JCT far upstream from the pore mouth. Thus, the solution becomes less valid as the JCT becomes very thick ($L \gg a$ and $L \gg b$). This additional flow resistance can be approximated to be $R_0 = \mu L/KA$ (one-dimensional Darcy's law). Multiplying this by Q to find the additional pressure drop and adding this to (7) yields:

$$\Delta P = \frac{\mu Q}{4Ka}\left(1 + \frac{4L\epsilon}{\pi a}\right) \tag{8}$$

Note that equation (8) indicates that if

$$\epsilon < a/4L \tag{9}$$

the extra pressure drop due to the pores will be a dominant effect.

Using equation (8), and the definition of the enhancement factor E, we find that:

$$E = 1 + \frac{\pi a}{4\epsilon L} = 1 + \frac{1}{4naL} \tag{10}$$

Predictions from this approximate analytic result were compared to data from the numerical simulation.

Results

Numerical solution of equations (3) and (4) yields the velocity and pressure distribution in the JCT for the typical parameter values given in Table 1. Figure 2

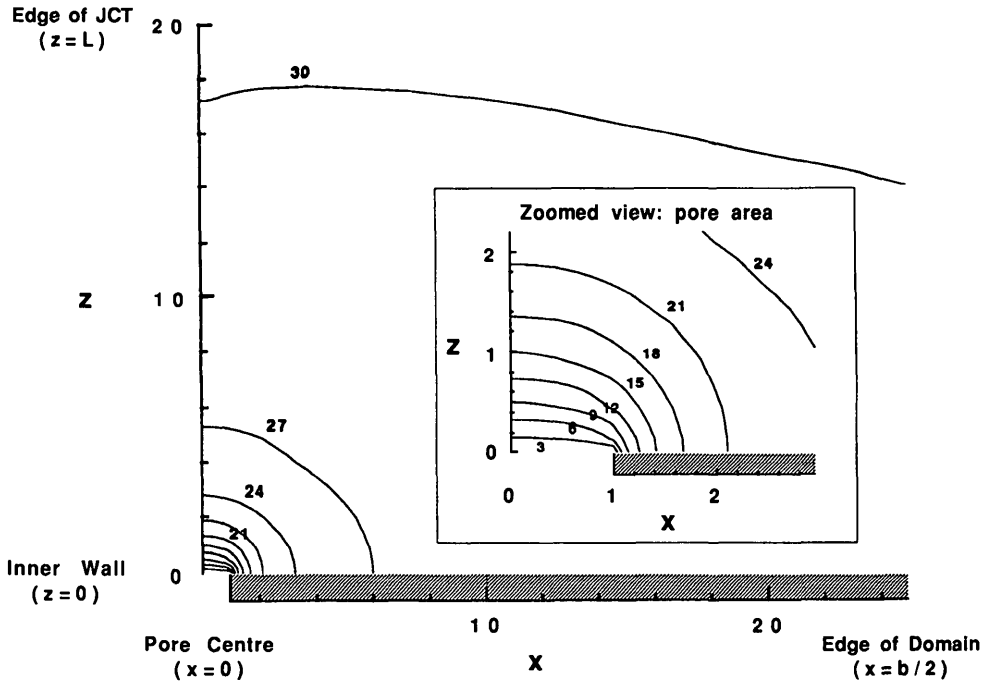

Fig. 2. Normalized pressure contours in the JCT in the neighborhood of a pore. The parameters used were the typical set of values shown in Table 1; the pressure at the entrance to the JCT (z = L) was 31.2. The length scales are normalized by the pore radius. The shaded area represents the inner wall.

shows the normalized pressure distribution in the JCT for the typical parameter values given in Table 1. One important feature of these results is that most of the pressure drop occurs within 3 pore radii of the pore mouth. Note also the magnitude of the total normalized pressure drop. It is approximately 30 times that which would occur if the flow were not forced to funnel through the small pore. The pressure remains near this value (31.2) throughout most of the JCT. Only in the neighborhood of the pore does the pressure decrease significantly. The velocity distribution in the JCT for this case (data not shown) exhibits high velocities only in the vicinity of the pore. Throughout the remainder of the JCT, the fluid velocities are small and, at z = L, nearly uniform.

In Figure 3, we plot the resistance enhancement factor E as a function of interpore spacing (b/L) and pore radius (a/L). Note that E is significantly greater than 1 except when $b/L \ll 1$ (high inner wall pore density or thick JCT). For the parameters typical of the normal human eye, the enhancement factor is approximately 30.

Also shown in Figure 3 is a comparison of the analytic limit for very small pore size ($a \ll L$, $a \ll b$; equation [10]) with the numerical calculations. The agreement is excellent, with enhancement factors always falling within 2% of the value determined from the numerical simulation for a/L < 0.1 and a/b < 0.1.

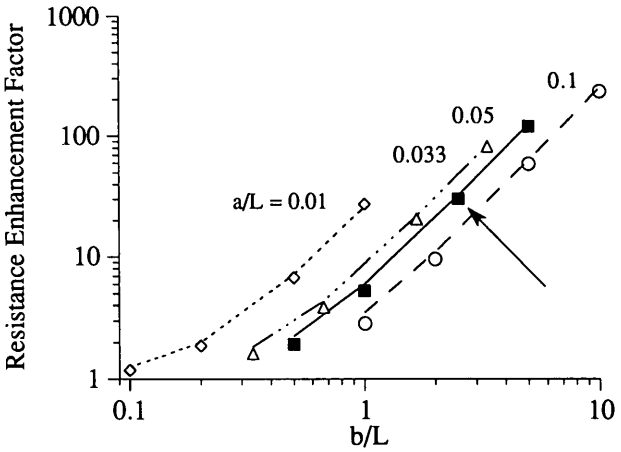

Fig. 3. Graph of the resistance enhancement factor (E: flow resistance of JCT/pore combination relative to that of JCT alone) as a function of b/L (ratio of interpore spacing to JCT thickness) for various values of a/L (ratio of pore radius to JCT thickness). The data points are from the numerical solution (NEKTON), whereas the lines are the approximate predictions from equation (10). The arrow points to the result from the set of typical values specified in Table 1.

Discussion

Hamanaka and Bill[9,17] observed that following use of a chelating agent or a proteolytic enzyme, ruptures of the inner wall endothelium were produced that changed outflow resistance by an amount greater than could be accounted for by the apparent flow resistance of the inner wall pores. Furthermore, following closure of the inner wall ruptures, the resistance quickly returned to baseline values. Grierson et al[18] demonstrated that the reduced outflow resistance as a result of pilocarpine in the primate eye was associated with an almost three-fold increase in the inner wall pore number. These observations led us to consider the potential for an interactive effect in which the nonuniform flow within the JCT caused by the low porosity of the inner wall endothelium might amplify the effective flow resistance of this region.

Using a simplified but physically realistic model, we examined the influence of inner wall pores on the JCT flow resistance. The results were dramatic: The flow resistance of the JCT was increased 30-fold by funneling effects due to the pores. This increase was not due to the flow resistance of the inner wall pores themselves. Rather, the increased flow resistance was the result of a decrease in the effective area through which the fluid must flow (as opposed to an increased lateral distance through which the fluid must pass). We were further able to determine a simple relationship (equation [10]) that allowed us to easily estimate the magnitude of this effect as pore number (n) or size (a) change.

This finding must alter the interpretation of previous examinations of JCT flow resistance[3,4] that did not account for the interaction between the JCT and inner wall pores. Results from our model suggest that the flow through the JCT is highly nonuniform. The conclusion regarding whether or not the electron lucent spaces in this tissue are gel-filled will need to be reexamined based on this new information. Our results suggest, at a minimum, that far less flow resistance than previously thought is required in the spaces of the JCT, whether open or gel-filled, to generate a significant pressure drop.

Several limitations of this analysis should be mentioned. First, we have assumed that the pores seen in micrographs of the inner wall endothelium are relatively static, open structures. If the process of vacuole filling and emptying is dynamic, so that at any given time some vacuoles are in a filling phase while others (those with pores) are in an emptying phase, the flow through the JCT would be more uniform than indicated by our model and the "funneling effect" would be diminished. Second, the analysis assumes that the JCT has a uniform permeability, even in the regions closest to the inner wall, including the vacuoles them-

selves. As the effects of "funneling" are manifest in the vicinity of the pores, open spaces in this region also will diminish the "funneling effect." In a related study, Ethier et al[3] considered the effects of JCT nonuniformity in their permeability model and found JCT heterogeneity to have a minimal effect on overall flow resistance.

It also has been assumed that the pores are of uniform size and are uniformly spaced over the inner wall endothelium. For low porosity ($a/b \ll 1$), it can be shown that the distribution of pore spacing will have a negligible effect on overall flow resistance, although nonuniform pore distributions certainly will give rise to significant variability in regional flow. Similarly, while the distribution of pore sizes that exist in the inner wall endothelium will create regional flow variations, the overall flow resistance can be computed using an appropriate mean value for pore radius.

As the aqueous humor passes through the pores of the inner wall of Schlemm's canal, there may be only a small pressure drop. However, the distant spacing of these pores leads to funneling of the flow of aqueous humor through the juxtacanalicular connective tissue in the region of the pores and greatly increases the flow resistance of this region. Because the bulk of the enhanced pressure drop occurs near the pores, the JCT in the proximity of the pores will have greatly increased importance in regard to outflow resistance, and the pores themselves may modulate this resistance. Histologically, the proximity of extracellular materials to the pores, such as plaque material found in the JCT and shown to be increased in primary open angle glaucoma,[19] will need to be examined. Furthermore, reports have indicated there is a significant decrease in the number of pores in the inner wall endothelium in primary open-angle glaucoma.[20] Our calculations indicate that the effective JCT flow resistance will be inversely proportional to inner wall pore density, so this could have important implications for the pathogenesis of primary open-angle glaucoma.

Appendix

We define our domain to extend throughout the unit cell shown in Figure 1, with the origin placed at the center of the pore. Let x and y represent the cross-sectional coordinates and r represent the radial location. To solve equation (2), we require a specification of pressure or its gradient on all surfaces of the computational domain shown in Figure 1. The appropriate boundary conditions become:

$$P(x, y, z = L) = P_{sc} + \Delta P \qquad \text{(A1)}$$

$$P(r < a, z = 0) = P_{sc} \qquad \text{(A2)}$$

$$\frac{\partial P}{\partial x}(x = \pm b/2, y, z) = 0 \qquad \text{(A3)}$$

$$\frac{\partial P}{\partial y}(x, y = \pm b/2, z) = 0 \qquad \text{(A4)}$$

$$\frac{\partial P}{\partial z}(r > a, z = 0) = 0. \qquad \text{(A5)}$$

(A1) and (A2) set the pressure drop through the system, with (A1) specifying uniform pressure at the entrance to the JCT and (A2) specifying uniform pressure at the pore. Conditions (A3), (A4), and (A5) specify zero fluid flux through the other boundaries of the system.

Key words: aqueous outflow resistance, juxtacanalicular connective tissue, inner wall of Schlemm's canal, hydrodynamic, porous media, aqueous outflow, pores

Acknowledgments

The authors acknowledge the motivation for this study provided by suggestions from Dr. David Epstein of the Department of Ophthalmology, University of California School of Medicine, San Francisco, California.

References

1. McEwen WK: Application of Poiseuille's law to aqueous outflow, AMA Arch Ophthalmol 60:290, 1958.
2. Johnson M and Kamm RD: The role of Schlemm's canal in aqueous outflow from the human eye. Invest Ophthalmol Vis Sci 24:320, 1983.
3. Ethier CR, Kamm RD, Palaszewski BA, Johnson M, and Richardson TM: Calculations of flow resistance in the juxtacanalicular meshwork. Invest Ophthalmol Vis Sci 27:1741, 1986.
4. Seiler T and Wollensak J: The resistance of the trabecular meshwork to aqueous humor outflow. Graefes Arch Clin Exp Ophthalmol 223:88, 1985.
5. Bill A and Svedbergh B: Scanning electron microscopic studies of the trabecular meshwork and the canal of Schlemm—an attempt to localize the main resistance to outflow of aqueous humor in man. Acta Ophthalmol 50:295, 1972.
6. Moses RA: Circumferential flow in Schlemm's canal. Am J Ophthalmol 88:585, 1979.
7. Mäepea O and Bill A: The pressures in the episcleral veins, Schlemm's canal and the trabecular meshwork in monkeys: Effects of changes in intraocular pressure. Exp Eye Res 49:645, 1989.
8. Rosenquist R, Epstein DL, Melamed S, Johnson M, and Grant WM: Outflow resistance of enucleated human eyes at two different perfusion pressures and different extents of trabeculotomy. Curr Eye Res 8:1233, 1989.
9. Hamanaka T and Bill A: Morphological and functional effects of Na_2EDTA on the outflow routes for aqueous humor in monkeys, Exp Eye Res 44:171, 1987.
10. Ethier CR and Kamm RD: The hydrodynamic resistance of filter cakes. Journal of Membrane Science 43:19, 1989.

11. Scheidegger AE: The Physics of Flow through Porous Media, 3rd ed. Toronto, University of Toronto Press, 1974.
12. NEKTON User's Guide, Version 2.7β, Nektonics, Inc., Cambridge, MA, 1990.
13. Grierson I and Lee WR: The fine structure of the trabecular meshwork at graded levels of intraocular pressure. Exp Eye Res 20:505, 1975.
14. Johnson M: Transport Through the Aqueous Outflow System of the Eye, Appendix B, Ph.D. thesis. Massachusetts Institute of Technology, 1986.
15. Levick, JR: Flow through interstitium and other fibrous matrices. Q J Exp Physiol 72:409, 1987.
16. Landau LD and Lifshitz E: The Classical Theory of Fields, 4th rev English ed. Oxford, Pergamon Press, 1975.
17. Hamanaka T and Bill A: Effects of alpha-chymotrypsin on the outflow routes for aqueous humor. Exp Eye Res 46:323, 1988.
18. Grierson I, Lee WR, Moseley H, and Abraham S: The trabecular wall of Schlemm's canal: A study of the effects of pilocarpine by scanning electron microscopy. Br J Ophthalmol 63:9, 1979.
19. Lütjen-Drecoll E, Futa R, and Rohen JW: Ultrahistochemical studies on tangential sections of trabecular meshwork in normal and glaucomatous eyes. Invest Ophthalmol Vis Sci 21:563, 1981.
20. Allingham RR, de Kater AW, Shahsafaei A, and Epstein DL: Relationship between outflow facility and giant vacuoles of Schlemm's canal in normal and glaucomatous human eyes. Invest Ophthalmol Vis Sci 31(Suppl):338, 1990.